

Ballistic Protection of Military Shelters from Mortar Fragmentation and Blast Effects using a Multi-layer Structure

T. Elshenawy^{#,*}, Mohamed Aboel Seoud[#], and G.M. Abdo[@]

[#]Technical Research Center, Cairo, Egypt

[@]Faculty of Engineering and Technology, Badr University in Cairo, Cairo, Egypt

^{*}E-mail: tamerhenawy@yahoo.com

ABSTRACT

In addition to its usage as a top attack ammunition in the battle field against troops, 120 mm mortar bomblet has been recently used in the terror attacks against military shelters and civil constructions. This research studies the protection of vehicle and personnel military shelters against mortar fragmentation warhead projectile and its destroying effects. The mortar warhead threat combines both blast load and ballistic fragment penetration effects. Composite structure layers are proposed herein to be integrated with concertina walls to achieve full protection against the mortar projectile destroying effects. The current paper investigates the ability of the proposed layers to stop the mortar's fragments and to mitigate its blast load. The velocity and the mass distribution of the produced projectile fragments were estimated using Split-X software. Besides, the ability of the proposed protection layers to stop the fragments and mitigate the blast wave was evaluated using AUTODYN hydrocode. A static firing test was then performed to validate the theoretical results and verify the effectiveness of the proposed protection added layers. The current study showed that the proposed composite layers are sufficient to protect the military shelters from the mortar's destroying ballistic effects.

Keywords: Mortar; Protection; Split-X; AUTODYN

1. INTRODUCTION

The continuous development in the various ammunitions in the main battle fields led to the developments of advanced energetic explosive materials¹⁻⁴ and its accompanied destructive effect as well as the ballistic threat containing the directed energy devices such as shaped charges, blasting charges and dual purpose fragmenting charges. As a result, mortar bombs have become more efficient in the current battle fields, military missions and terror attacks. The concertina units have become the most popular means for protecting military personnel and facilities against ballistic and fragmentation penetration. They have been extensively used in the protection of personnel, vehicles, equipment, and facilities in military, peacekeeping, and humanitarian and civilian operations. Concertina units are currently in use with many military armies and organizations including the NATO and UN troops⁵. Concertina is a prefabricated, multi-cellular system, made of nonwoven polypropylene geotextile encapsulated in a steel welded mesh and filled with sand. Multiple threats have been found to affect this concertina units and military shelters such as blast loading⁶⁻⁸ and ballistic penetrations⁹⁻¹¹. One of these threats that has severe dual damage effect is the mortar bomblet projectile. This mortar has been recently used in many terror attacks in Sinai Peninsula against army shelters and civil buildings. General specifications of this threat (projectile) are as listed in Table 1. The dual effect of the mortar fragmentation warhead

includes both the intensive fragment mass distribution and the blast load generated from the detonation of the explosive charge that was found to have considerable effect on the personnel and concertina vehicle shelters when fired from mortar barrels. Various studies have been performed on the fragmentation pattern of this mortar bomblet. Zecevic¹², *et al.* investigated the variation of the fragment mass distribution versus the age the bomblet's body was manufactured. However, limited studies have been performed on the blast load result from the detonation of mortar rounds and the necessary composite layers needed to mitigate the blast load and to stop the generated penetrating fragments.

Table 1. Technical data of the studied mortar fragmentation warhead¹³

Property	Specification
Total Mass	12.6 kg
Explosive mass (TNT)	2.25kg
Caliber	120 millimetres (4.7 in)
Casing	Steel 9189VP(JAS)
Fuze	Impact, Super quick, and delayed action

2. CONTRIBUTION OF THE CURRENT RESEARCH

The main objective of the current research is to propose a composite structure that can protect the military shelters against the mortar effects. To achieve this goal, theoretical studies along with experimental investigation including the ability of

the proposed structure to resist the fragments and blast loading were implemented. The current study includes the following research activities:

- Studying the mortar fragmentation using CONDAT Split-X software
- Simulation of the fragments penetration into the proposed structural elements via Autodyn-3D hydrocode
- The blast load interaction with the proposed composite structure using Autodyn-3D hydrocode
- Full scale testing program to verify the workability of proposed composite structure and to ensure its reliability against the tested ballistic threat.

3. PROPOSED PROTECTION LAYERS

The proposed protection structure consists of five composite layers. The first (lowest) layer consists of arched steel beams covered by polypropylene geotextile. The second layer is a sand layer with variable depth (optimised during experimental testing). The third layer is an aluminum-polyurethane foam sandwich layer that is 5 cm thick. The fourth layer is a 30 cm sand layer. The last (top) layer is a sandwich of V shaped steel beams and plates. The proposed protection structure is as illustrated in Fig. 1.



Figure 1. Proposed protection layers against mortar warhead.

4. EXPERIMENTAL TESTING PROGRAM

A static firing test of the mortar warhead was performed to validate the analytical/numerical estimations and investigate the efficiency of the proposed protection structure to mitigate the blast load of the explosion and fragmentation effects. The static firing was performed by detonating the bomblet on the top left of the proposed protection structure using an electrical detonator instead of the existing mortar's mechanical impact fuze as shown in Fig. 1.

5. SPLIT-X FRAGMENTATION CALCULATIONS

The fragmentation behavior of the mortar's shell casing has been studied by many researchers. The previous studies investigated the fragments' distribution pattern, mass, and velocity in addition to the blast loading of the warhead¹⁴⁻¹⁸. In the current study, the mortar fragments' distribution pattern, mass, and velocity were estimated using SPLIT-X software developed by CONDAT¹⁹. Considering it's built in material library, SPLIT-X enables the designer to assess the performance of a certain warhead fragmenting design if the basic geometry and design material were assigned to this warhead.

The mortar projectile has a thick shell in order to produce massive fragments and to afford both the high pressure (200 MPa)³⁰ and the elevated temperature (2000 °C)²¹⁻²² inside the mortar barrel. Although this temperature is much higher than the ignition temperature of the most of the explosives, the thick shell is still needed to achieve the desirable destructive effect.

6. ANSYS AUTODYN 3D SIMULATION

AUTODYN-hydrocode is a numerical finite difference code that is based on the three conservation equations; mass, momentum and energy, in which a material is defined by its equation of state (EOS) and its strength model²³. This software has several applications in calculating the penetration depth of shaped charge jets into different target materials²⁴. It has been also used in the study and the assessment of the fragmentation pattern of fragmenting warheads and showing the metal-explosive interaction and the analysis of the produced data of calculated metal fragments²⁵. In the current paper, AUTODYN-3D was used to analyse the fragments evolved from the detonation of 120 mm projectile. Besides, it was also used to simulate the interaction of the mortar's largest kinetic energy fragments with the proposed protection structure. Moreover, it was used to simulate the effect of the bomblet's blast loading on the proposed composite protection layers. In the following subsections, the simulation of both the fragments' penetration and the blast loading are briefly discussed.

6.1 Materials Modelling

The explosive charge filling the mortar projectile is TNT with a loading density of 1.63 g/cm³. EOS of this explosive material is 'Jones-Wilkins-Lee' (JWL)²⁶⁻²⁷, with constants determined by the cylinder expansion test and as listed in Table 2 for TNT material²⁸.

Table 2. The JWL parameters of the TNT charge material.

Parameter	TNT
Density (g/cm ³)	1.630
Parameter A (kPa)	3.740×10 ⁸
Parameter B (kPa)	3.747×10 ⁶
Parameter r_1	4.15
Parameter r_2	0.9
Detonation velocity (m/s)	6930
Energy/volume (kJ/m ³)	6.00×10 ⁶
C-J-pressure (kPa)	2.1×10 ⁷
Parameter ω (-)	0.3

The mortar's shell was modeled as steel 1006, while the target's steel was modelled as steel 4340. Shock EOS was used for the warhead's steel, the target's steel, the aluminum layer, and the foam materials. Shock EOS is explained in details in other references^{23,30}. The strength model selected for steel materials was Johnson-Cook²⁹, while no strength model was assigned for the aluminum and foam materials. The mechanical properties and the material model constants are as listed in

Table 3 for the used materials. The constants' values were taken exactly as found in the AUTODYN library.

The equation of state of the sand material is 'compact' in which various pressure values and corresponding material densities were entered into material library together with the relevant sound speed at each density. 'MO Granular' strength model has been selected for the sand material, which was also described by the Drucker-Prager model. This model is both density and pressure dependent model, in which the maximum yield surface is determined using tri-axial shear tests. Accordingly, it determines whether a material has failed or undergone plastic yielding. Besides, the compacted material hardening and accompanied variations in the shear modulus with density are also estimated by this model. The interested reader can refer to the Autodyn theory manual²³ for more details about both strength models.

6.2 Penetration Simulation

The fragments' interaction (penetration) with the target's composite layers was simulated using Lagrange method, in which the moving Lagrange fragment grid impacts the multilayered Lagrange targets as illustrated in Fig. 2. Lagrange-Lagrange interaction was defined between the fragments and the target surfaces. Detailed description of this interaction was introduced in previous studies^{31,32}. Only three identical fragments of the highest kinetic energy were included in the model. The initial condition of this numerical simulation was the impact velocity of the fragment. This velocity was estimated via the Split-X code to be 1100 m/s.

6.3 Blast-protection Structure Interaction

A two-step numerical simulation was executed to study the effect of the mortar explosion on the proposed protection

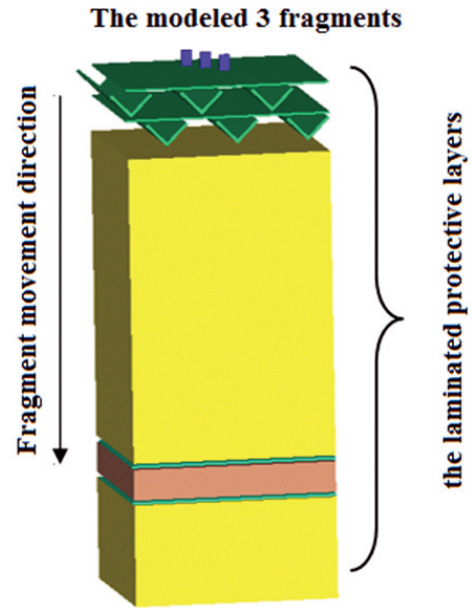


Figure 2. Modelling of fragment/protection layers interaction via AUTODYN-3D.

layers. In the first step, the blast wave generated from the explosion of 2.25 Kg TNT in free air was simulated via one-dimensional (1-D) axial-symmetry analysis. In this step, Euler method was used to compute the pressure-load history; Fig. 3(a). In the second step, the 1-D analysis (containing the pressure and time values) was remapped into 3-D Euler-Lagrange interaction model. In Autodyn, the Euler-Lagrange interaction (which represents fluid-structure interaction) couples the Eulerian domain to the Lagrangian structural domain. Subsequently, this model was used to mimic the interaction between the generated blast wave and the proposed protection structure. In this scheme, a Lagrangian structural domain represented the steel and aluminium-polyurethane foam layers, whereas Eulerian domain represented the TNT and sand layers; Fig. 3(b). Only a representative section (40 cm x 40 cm) of the laminated structure was included in the model to reduce the computational effort. Subsequently, a transmit boundary condition was applied to the Lagrangian parts, while 'flow out' boundary condition was assigned to the Eulerian parts. To better investigate the interaction between the blast wave and the composite layers, several gauges were positioned at the middle of the composite layers. Gauges 1 and 2 were placed in the steel plates, gauges 3 and 6 were added to the aluminium plates, gauges 4 and 5 were positioned through the foam layer, gauges 7 and 8 were placed at the top and mid of the upper sand layers, and gauge 9 was located at the bottom of the lower sand layer, as illustrated in Fig. 3(b).

Table 3. The model parameters of the fragment and target materials used in simulation²³

Parameter	Steel 1006	Steel 4340	Al2024	Polyurethane foam
Equation of state	Shock	Shock	Shock	Shock
Reference density (g/cm ³)	7.89	7.75	2.785	1.265
Gruneisen Coefficient	2.17	2.17	2.00	1.55
Parameter C ₁ (m/s)	4569	4569	5328	2486
Parameter s ₁ (none)	1.49	1.49	1.338	1.577
Ref. temperature (K)	300	300	300	300
Strength model	JC	JC		
Constant A (kPa)	8.18×10 ⁷	7.70×10 ⁷	-	-
The hardening constant B (kPa)	3.5×10 ⁵	7.92×10 ⁵		
Hardening exponent; n (-)	0.36	0.26		
Strain rate constant (-)	0.022	0.014		
Thermal softening exponent (-)	1	1.03	-	-
Melting temperature T _m (K)	1811	1793		
Ref. strain rate (1/s)	1	1		

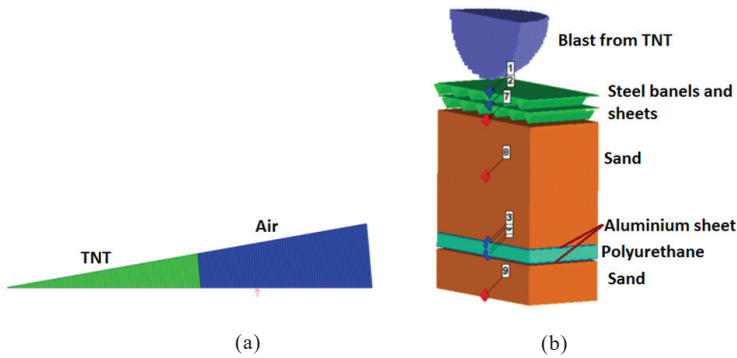


Figure 3. (a) 1-D simulation of 2.25 Kg TNT explosion in air and (b) 3-D simulation of the blast wave-proposed protection structure interaction.

7. RESULTS ANALYSIS

7.1 Fragmentation Pattern, Distribution and Velocity

Samples of the output from the SPLIT-X software for a mortar grenade are as illustrated in Figs. 4 and 5. The results demonstrated that the fragment that produced the maximum kinetic energy was 6.2 gm. The velocity of this fragment along with its radial displacement from the bomblet (threat) axis are

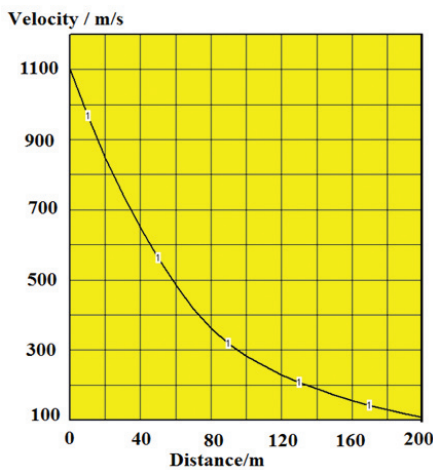


Figure 4. The velocity-distance history of the 120 mm mortar largest kinetic energy fragment.

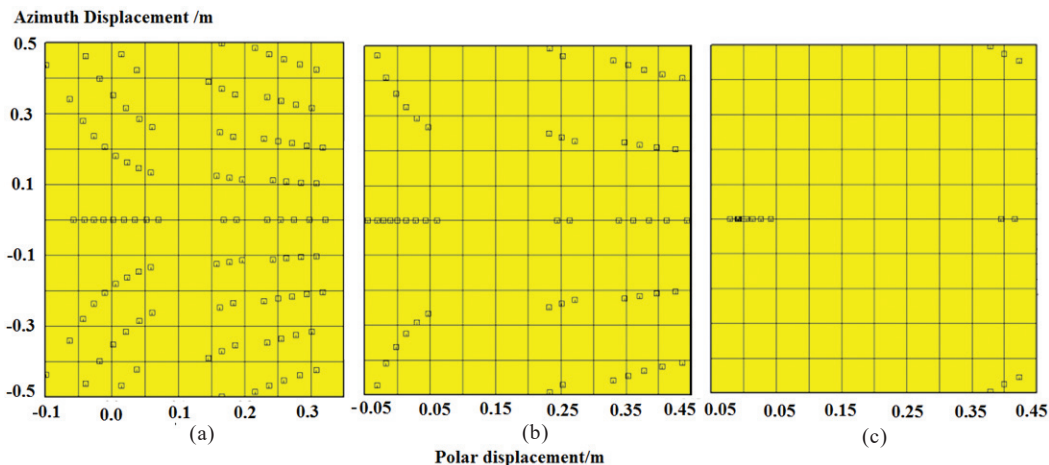


Figure 5. Fragment impact distribution at different distances from the projectile axis on a target with an area of 1 m²; (a) 1 m (104 hits), (b) 2 m (56 hits), and (c) 4 m (17 hits).

as illustrated in Fig. 4. At the moment of detonation, the initial velocity of such fragment was found to be 1100 m/s. This velocity decreased dramatically to 850 m/s at 20 m and 650 m/s at 40 m.

The fragment’s lethal threshold and the effective hitting area of humans have been discussed in details by Cuadros³³. The probability of hitting a human being by the generated fragments can be obtained from Fig. 5 by considering the area of an adult to be one square meter (height = 2 m, width = 0.5 m). The hitting probability of the studied mortar (threat) showed 104 hits, 56 hits and 17 hits at distances of 1 m, 2 m and 4 m, respectively from the detonation point.

7.2 Mortar-structure Interaction

The static firing test revealed that the fragments were able to perforate only the first (steel) layer. However, no perforation through the remaining layers was observed (Figs. 6 and 7). The experimental test also clarified that the blast of the mortar (threat) resulted in a deformation in the steel layers along with compaction in the upper sand layer (30 cm thick).

The analytical / numerical simulations are in a reasonable agreement with the experimental investigations. The fragments-proposed layers interaction at different times from the moment of impact is illustrated in Fig. 8. This simulation predicted the fragments’ perforation to be confined to the steel layers as observed experimentally. However, a difference between the numerical predicted perforation area (by AUTODYN) and the experimental measured one is clear. This can be attributed to the limited number of fragments (only 3 fragments) included in the theoretical numerical simulation, whereas, a large number of fragments interacted with the target in the real firing test. Another factor that might have contributed to this difference is the fact that the fragments penetration effect was combined together with the blast wave effect during the experiment. Whereas, the two effects were studied separately in the preliminary theoretical analyses.

After performing the static firing test, a rope was attached at the beginning and the end of the top left edge of the first (steel) layer to measure the composite layers’ deflections. These locations (the beginning and the end of the left edge) were

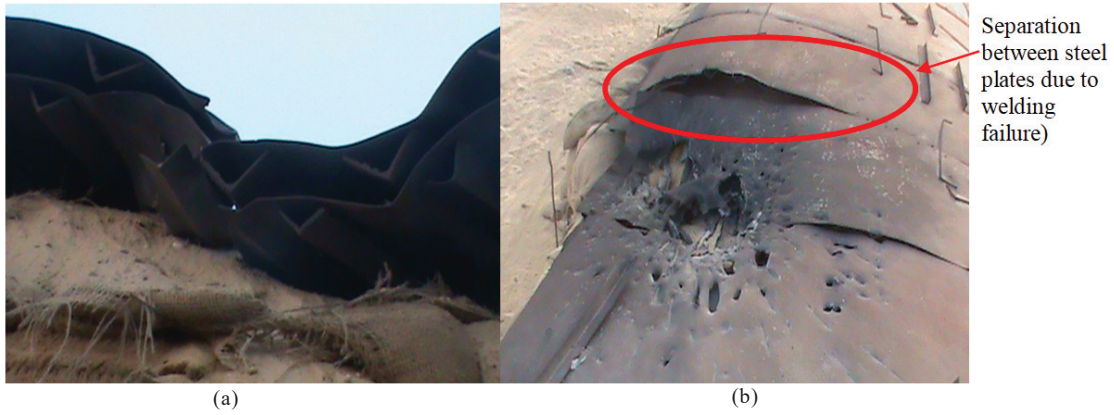


Figure 6. The protection layers from outside after performing the static firing test: (a) elevation view and (b) plan view.



Figure 7. The shelter from inside (neither fragment penetration was recorded nor significant deformation under the blast loading was observed).

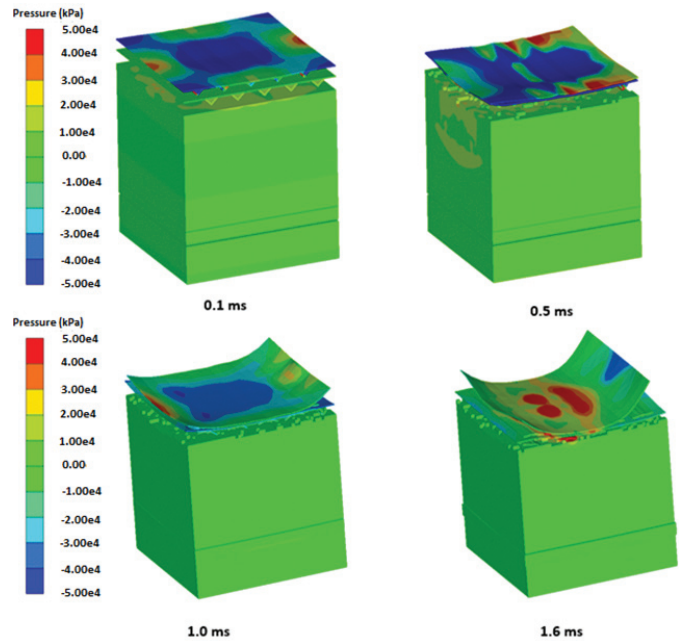


Figure 9. The blast loading-target interaction.

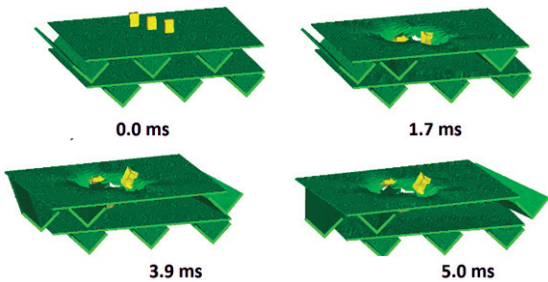


Figure 8. The fragment / target interaction (sand, aluminium and foam materials are not shown).

clearly observed to be neither affected by the mortar's fragments nor its explosion. Subsequently, the rope was considered as a reference line to approximately measure the layers' deflections. A comparison among the measured and estimated deflections at different locations through the protection layers is as listed in Table 4. The simulated interaction of the target-blast loading at different times from the moment of detonation is as illustrated Fig. 9. While, the deflection history of five gauges obtained from the numerical simulation is displayed in Fig. 10. The simulation results clarified that the 10 cm sand layer was compacted for about 11 mm under the blast loading effect (G6 and G9). Similarly, the simulation illustrated that the 5 cm foam

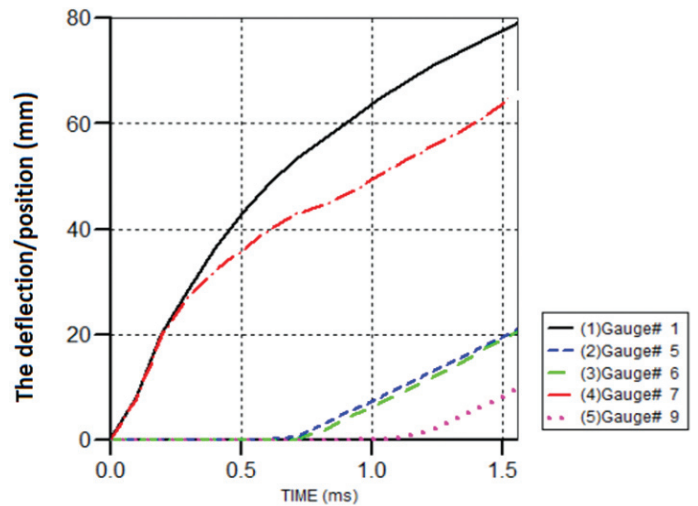


Figure 10. The deflection under the blast loading.

Table 4. The measured and estimated deflections through the protection layers

Gauge number	Gauge location	Measured deflection (mm)	Estimated deflection (mm)	Error percentage
G1	Top of the steel layer	120	80	33
G3	Top of the aluminum sandwich layer (bot. of the upper sand layer)	—	26	—
G6	Bot. of the aluminum sandwich layer (top of the lower sand layer)	—	21	—
G7	Top of the upper sand layer	90	65	28
G9	Bot. of the lower sand layer	13	10	23%

layer was compacted for about 5mm due to the explosion effect (G3 and G6), the 30 cm sand layer was predicted to compact for about 39 mm (G3 and G7), whereas the steel layers were estimated to deform vertically for about 15 mm (G1 and G7). These results indicate that the blast wave transferred through the whole layers and demonstrate that all the layers contributed to the mitigation of the blast load.

The maximum measured deflections at different locations were found to be always greater than the estimated deflections via the hydrocode simulation at the same locations. The error in the estimated errors ranged from 23 per cent - 33 per cent (Table 4). These differences can be attributed to the breakage in the welding between the plates as it is as illustrated in Fig. 6. This welding failure resulted in a rigid motion of the separated steel layers, hence increasing the deflection through the protection layers in the real structure.

8. SUMMARY AND CONCLUSIONS

Composite protection layers have been proposed to protect military shelters and bunkers from mortar warhead destroying effects. The proposed structure consisted of five layers combining steel, sand, and aluminium-polyurethane foam sandwich panel. The effect of both the blast and the fragmentation accompanied with this mortar on the proposed protection layers was studied numerically and experimentally. The numerical simulation results predicted via Autodyn-3D hydrocode were found to be in acceptable agreement with the experimental measured results. The experimental firing test and the numerical simulation clarified that all the composite layers contributed to the mitigation of the blast loading of the mortar warhead, whereas the fragmentation effect was confined to the first layer. Both the experiment and the simulation proved that the proposed protection structure is able to mitigate the generated blast load and to stop the fragments of this mortar threat.

REFERENCES

1. Elshenawy, T.; Elbeih, A. & Klapötke, T. A Numerical method for the determination of the virtual origin point of shaped charge jets instead of using flash X-ray radiography. *J. Energetic Mater.*, 2018, **36**(2), 127-140. doi.org/10.1080/07370652.2017.1324532.
2. Elbeih, A.; Elshenawy, T.; & Gobara, M. Application of cis-1,3,4,6-Tetranitrooctahydroimidazo-[4,5d]imidazole (BCHMX) in EPX-1 Explosive. *Def. Sci. J.*, 2016, **66**(5), 499-503. doi: 10.14429/dsj.66.9876.
3. Elshenawy, T. Determination of the velocity difference between jet fragments for a range of copper liners with different small grain sizes. *Propellants, Explos. Pyrotech.*, 2016, **41**(1), 69-75. doi: 10.1002/prop.201500095.
4. Elshenawy, T. & Li, Q. M. Breakup time of zirconium shaped charge jet. *Propellants, Explos. Pyrotech.*, 2013, **38**(5), 703-708. doi: 10.1002/prop.201200191.
5. Szabó, S.; Tóth R. & Kovács, Z. Force protection solutions with HESCO bastion concertainer. *AARMS: Academic Applied Res. Military Sci.*, 2011, **10**(1), 31.
6. Li, Q. & Meng, H. Pressure-impulse diagram for blast loads based on dimensional analysis and single-degree-of-freedom model. *J. Eng. Mech.*, 2002, **128**(1), p. 87-92. doi: 10.1061/(ASCE)0733-9399(2002)128:1(87)
7. Luccioni, B.; Ambrosini, D. & Danesi, R. Blast load assessment using hydrocodes. *Engineering Structures*, 2006, **28**(12), 1736-1744. doi: 10.1016/j.engstruct.2006.02.016.
8. Ngo, T., Mendis, P.; Gupta, A. & Ramsay, J. Blast loading and blast effects on structures—an overview. *Electronic J. Struct. Eng.*, 2007, **7**, 76-91.
9. Wen, H. Predicting the penetration and perforation of FRP laminates struck normally by projectiles with different nose shapes. *Composite structures*, 2000, **49**(3), 321-329.
10. Adel, B. Numerical approach in predicting the penetration of limestone target by an ogive-nosed projectile using Autodyn 3-D. In 12th Int. Colloquium on Structural and Geotechnical engineering, ICSGE. 2007, Egypt.
11. Daniels, A. S.; Baker, E. L., De Fisher, S. E.; Ng, K.W. & Pham, J. Bam Bam: large scale unitary demolition warheads. In Proceedings of the 23rd International Symposium on Ballistics, 2007, Tarragona, Spain.
12. Zecevic, B.; Catovic, A.; Terzic, J. & Kadic, S. S. Analysis of influencing factors of mortar projectile reproduction process on fragment mass distribution. In 13th Seminar on New Trends in Research of Energetic Materials, Part II. 2010.
13. Military factory "Unis Pretis d.d. Sarajevo" - Bosnia and Herzegovina, www.pretis.ba.
14. Mott, N. F. Fragmentation of shell cases. In Proceeding of the Royal Society, A mathematical, physical and engineering sciences. A 189.1018, 1947, pp.300-308. doi: 10.1098/rspa.1947.0042.

15. Sterne, T. A Note on the initial velocities of fragments from warheads. Ballistic Research Laboratories, BRL Report No. 648, September, 1947.
16. Grabarek, C. I. Fragmentation of single and double wall cylindrical warheads. Defense Technical Information Center, Report No. DTIC_AD0729316, November, 1951.
17. Henry, I.G. The Gurney formula and related approximations for the high-explosive deployment of fragments. Aerospace Group, Hughes Aircraft Corp., California, Report No. PUB-189, 1967.
18. Buchholz, J. R. Design, development, fabrication and testing program to demonstrate feasibility of the mass focus/fragmentation warhead, 1973.
19. Rottenkolber, E. "SPLIT-X V5." An expert system for the design of fragmentation warheads. User manual, CONDAT GmbH, Scheyern-Fernhag (2002).
20. PRODAS Team, 120 mm HE fragmentation Tutorial Prodas, 2006.
21. Toivola, J.; Seppo, M. & Henna-Riitta, J. Force, pressure and strain measurements for traditional heavy mortar launch cycle. *J. Struct. Mech.*, 2011, **44**(4), 309-329.
22. Matthew, F. Case study flow forming mortar cannon barrels, *Adv. Mater. Processes*. Report. Dynamic Flow form Corp. Billerica, Massachusetts, 2008.
23. Team, A. Autodyn theory manual. Century Dynamics: CA, 1997.
24. Elshenawy, T.; Elbeih, A. & Li, Q.M. A Modified penetration model for copper-tungsten shaped charge jets with non-uniform density distribution, *Cent. Eur. J. Energ. Mater.*, 2016, **13**(4), 927-943.
doi: 10.22211/cejem/65141.
25. Ugrčić, M. Numerical simulation of the fragmentation process of high explosive projectiles. *Sci. Tech. Rev.*, 2013, **63**(2), p.47-57.
26. Baudin, G. & Serradeill, R. Review of Jones-Wilkins-Lee equation of state. New Models and Hydrocodes for Shock Wave Processes in Condensed Matter, Paris, France, Edited by Laurent Soulard; *EPJ Web of Conferences*, 2010, **10**(10), 00021.
27. Lee, E.; Hornig, H. & Kury, J.; Adiabatic expansion of high explosive detonation products. 1968, California Univ., Livermore. Lawrence Radiation Lab (LLNL). USA, Report No. UCRL-50422. May, 1968.
doi: 10.2172/4783904
28. Lee, E.; Finger, M. & Collins, W. JWL equation of state coefficients for high explosives. Lawrence Livermore National Lab., (LLNL), CA, USA, Report No. UCID-16189. January, 1973] doi: 10.2172/4479737.
29. Johnson, G. & Cook, W. A. Constitutive model and data for metals subjected to large strains, high strain rates and high temperatures. In the 7th International Symposium on Ballistics, 1983.
30. AUTODYN Compendium of Papers, Century Dynamics Incorporated, 1991: USA.
31. Elshenawy, T. & Li, Q. Influences of target strength and confinement on the penetration depth of an oil well perforator. *Int. J. Impact Eng.*, 2013, **54**, 130-137.
doi: 10.1016/j.ijimpeng.2012.10.010
32. Team, A. Hands on examples, shaped charges jet formation and impacting on Brick walls. CA, USA. 2007.
33. Cuadros, J. Terminal ballistics of non-lethal projectiles, In 14th International Symposium on Ballistics, Quebec, Canada, 1993.

CONTRIBUTORS

Dr Tamer Elshenawy obtained his PhD from the University of Manchester, UK, in 2012. He has been working in the field of research in weapons, ammunition and explosives as well as rocket propulsion. Current researches including shaped charges design and developments as well as explosive manufacturing technologies.

In the current study, his contribution was Autodyn, split-X calculations and some of the experimental measurements.

Dr Mohamed Abdelkhalik Aboelseoud received his PhD in civil engineering from Missouri University of Science and Technology. Current researches including hybrid composite beam bridges, behavior and analysis of fiber reinforced polymer (FRP) composites, durability of FRP composites, blast mitigation, ballistic armours, electrically conductive cement-based materials, and structural analysis.

In the current study, his contribution was Autodyn calculations and supervision of the experimental trial design.

Dr G.M. Abdo received his PhD in Mechanical and Tribological Behavior of Ni-Mo Sintered Steel, from the Military Technical College, Egypt. Presently working as an Associate Professor in the Department of Mechanical Engineering, Faculty of Engineering and Technology, Badr University in Cairo, Cairo, Egypt. He was senior researcher at the Military Technical Research Centre, Cairo. He has contributed to several research projects in the field of material science, composite structure, design and implementation of mechanical systems, and protection systems.

In the current study, his contribution was the experimental measurements, design and assessment.